



Short communication

Catalytic performance of Pt film with dendritic structure for PEFC

Kazuhiro Yamada*, Kazuya Miyazaki, Shinosuke Koji, Yoshinobu Okumura, Masaaki Shibata

Canon Research Center, Leading-Edge Technology Research Headquarters, Canon Inc., 3-30-2 Shimomaruko, Tokyo 146-8501, Japan

ARTICLE INFO

Article history:

Received 8 January 2008
 Received in revised form 13 February 2008
 Accepted 16 February 2008
 Available online 29 February 2008

Keywords:

Polymer electrolyte fuel cell
 Sputter deposition
 Pt dioxide

ABSTRACT

A Pt catalyst film with dendritic microcrystalline structure has been prepared by reducing PtO₂ deposited by reactive sputtering. It is to be employed as the cathode catalyst of a polymer electrolyte fuel cell (PEFC). Despite using no support material, this dendritic Pt film exhibits a very low density of 3.3 g cm⁻³. When applying the dendritic Pt as the cathode catalyst layer for a single fuel cell, the dendritic Pt provided higher performance, larger electrochemical surface area (ECA) and improved diffusion characteristics compared to a conventional sputtered Pt film. The activity based on unit ECA of the dendritic Pt was higher than that of Pt/C.

© 2008 Elsevier B.V. All rights reserved.

1. Introduction

Solid polymer electrolyte fuel cells (PEFC) are expected to be a future energy-generation apparatus because of their high-energy conversion efficiency, cleanliness, and absence of noise. Conventionally, the catalyst is formed into fine particles and supported on carbon particles in order to increase the surface area and improve the catalyst utilization. However, in carbon supported catalysts, the oxidation of the carbon support, can lead to the agglomeration of the Pt nanoparticles and their detachment from the support [1,2]. The oxidation of the carbon support also causes the alteration of the pore structure and the loss of the hydrophobicity of the pore surface in the catalyst layer. Therefore, the oxidation of the carbon support degrades the performance and operation lifetime of PEFC.

Several works show Pt catalyst films without any support material deposited by sputtering [3–5]. Gruber et al. [6] investigated the performance of sputter-deposited catalyst films under a wide range of Pt loading. However, the films described in the above-mentioned publications are dense and have poor surface area in the case of high Pt loading. Further, increased Pt loading results in the decrease of mass activity, and high performances have not yet been obtained.

The scope of this paper is to investigate the effect of the morphologies and surface area of pure Pt catalyst films on PEFC performances.

2. Experimental

2.1. Preparation of catalysts and MEA (membrane and electrode assembly)

It is known that α -PtO₂ which is sometimes called Adam's catalyst, has a dendritic structure [7]. It is also known that α -PtO₂ films can be formed by the reactive sputtering deposition process [8–13]. Thus, in this study, the platinum dioxide (PtO₂) film with dendritic structure was deposited on the MPL (Micro porous layer) surface of a gas diffusion layer (LT1200W, available from E-TEK Div. of BASF Fuel cell Inc.) using reactive sputtering process under 100% O₂ partial pressure at room temperature. The RF power applied on the Pt target (4 in. diameter) and the total pressure in the deposition process were 1 kW and 5 Pa respectively. This is to obtain aPtO₂ film with a high surface area. After the sputtering process, the PtO₂ film was subjected to a hydrogen reduction treatment using 2% H₂/He (0.1 MPa) at room temperature to thereby obtain a Pt catalyst film. The obtained film was characterized by SEM/EDAX technique, Transmission Electron Microscopy (TEM), X-ray diffractometry (XRD), and X-ray Photoelectron Spectroscopy (XPS). A conventional Pt film was also sputtered with Ar plasma at 0.67 Pa on the MPL for comparison. The Pt loading of sputtered catalysts were 0.6 mg cm⁻². Nafion® solution (available from Sigma–Aldrich) was simply dropped on the Pt films as an ionomer, and the whole was dried at the ambient temperature to remove the solvent. The ionomer/Pt weight ratios of the samples were in the range of 6–8 wt%. A solid polymer electrolyte membrane (NRE212CS, available from DuPont) was sandwiched by the sputtered Pt catalyst film and platinum-supported carbon (Pt/C) catalyst layer (trade name: NMC C1-30, available from E-TEK, 30% Pt weight on carbon), and the whole was subjected to a pressure of 4 MPa

* Corresponding author. Tel.: +81 3 3758 2111; fax: +81 3 3757 3096.
 E-mail address: yamada.kazuhiro350@canon.co.jp (K. Yamada).

at 150 °C during 10 min to obtain the MEA. A conventional MEA, where the Pt/C catalysts were pressed on both side of electrolyte membrane, was also prepared for comparison.

2.2. Fuel cell performance measurements

A commercially available unit cell (FC-05-02, produced by Electrochem, Inc.) was used as a test cell in this study. Three-line serpentine flow field design was used in the carbon separator. The catalytic electrode area was 4 cm² (20 mm × 20 mm).

The sputtering Pt catalyst film was used as the cathode catalyst layer, and the Pt/C catalyst layer was used as the anode catalyst layer. The MEA and anode gas diffusion layer (LT1400W, available from E-TEK Div. of BASF Inc.) were sandwiched by carbon separators and metal corrector to thereby form a unit cell. Thus, LT1200W acted as the cathode gas diffusion layer in this test cell. LT1200W was also used as the cathode gas diffusion layer when using Pt/C as the cathode catalyst layer in the conventional MEA.

Galvano-dynamic measurements were carried out with a sweep rate of 1 mA cm⁻² s⁻¹ at 80 °C, while humidified H₂, Air and O₂ gases were supplied to the unit cell with flows of 200 ml s⁻¹. The cyclic voltammetry was also performed at a cell temperature of 40 °C, while humidified N₂ and H₂ gases were supplied to the cathode and anode respectively, to thereby obtain an electrochemical surface area (ECA) in the Pt catalyst layer.

3. Results

3.1. Characterization of the Pt catalyst film

The XRD pattern of the sputtered Pt oxide film is shown in Fig. 1. The diffraction peaks are broadened, and show very poor crystallinity. This is significant with the reported results of α -PtO₂ [7]. Only the two broad peaks like the amorphous phase are visible for the obtained Pt oxide film. The strongest peak ($2\theta = 34.2^\circ$) shows a good agreement with the literature data [7,11].

From XPS spectra, the binding energies (Eb) of Pt_{4f(7/2)} and Pt_{4f(5/2)} for the Pt oxide are 73.65 eV and 77.05 eV respectively, which is similar with the reported result of α -PtO₂ [7,8,10,12,13].

Fig. 1 also shows the XRD pattern of the reduced Pt film. The diffraction peaks of the reduced Pt film show a good agreement with the peaks of bulk platinum. The binding energies (Eb) of Pt_{4f(7/2)} of the reduced Pt film is equal to 70.7, which corresponds to bulk Pt. These results mean that the PtO₂ film is reduced by the

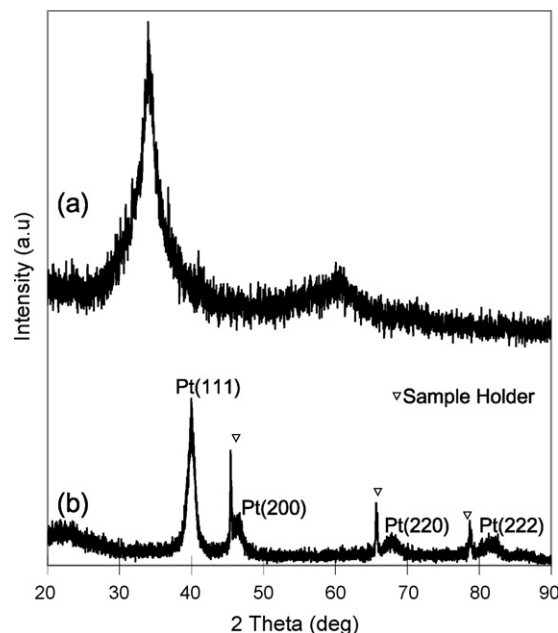


Fig. 1. XRD patterns of the Pt oxide film (a) as-deposited and (b) treated at room temperature in 2% H₂/He (0.1 MPa) flow for 30 min.

hydrogen reduction treatment. It is not clear why the film is reduced at room temperature, because bulk PtO₂ is usually not reduced at room temperature. The obtained PtO₂ film may be unstable. Judging from the features represented by the (1 1 1) diffraction peak of the reduced Pt film and the peak width at half intensity (Scherrer treatment), the crystalline size in the reduced Pt catalyst is estimated at about 10 nm.

The SEM micrographs of the as-deposited Pt dioxide and the reduced Pt film are shown in Fig. 2 (a) and (b) respectively. It is found that the dendritic structure is maintained despite a volume diminution occurred during the reduction process. Fig. 3 shows the TEM micrograph of the cross-section of the dendritic Pt film in the MEA. From a careful TEM observation, its Pt grain size was found to be ca.10 nm, similar to the result estimated by XRD. Fig. 3 also shows that the observed continuous pores in the direction of the film thickness may act advantageously to facilitate substance transport in the fuel cell. The density of the dendritic Pt film is easily calculated from the weight of Pt and its thickness. The den-

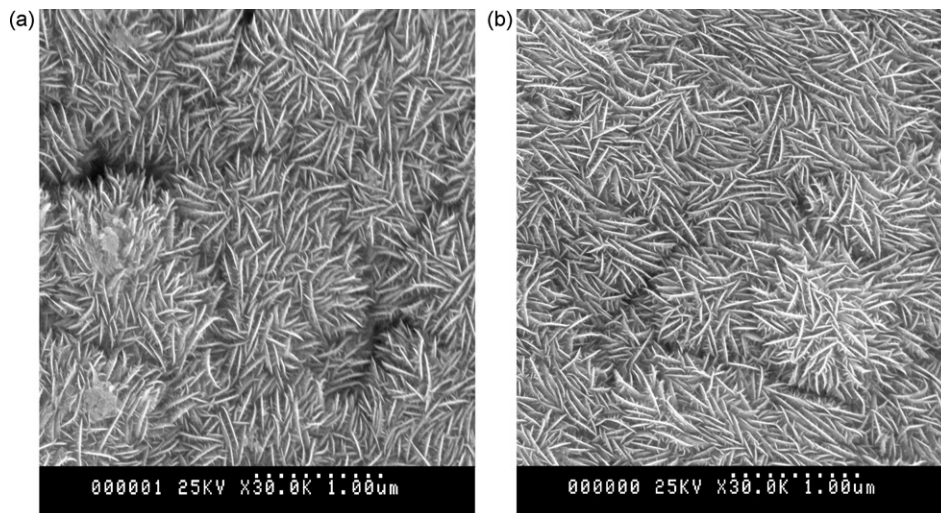


Fig. 2. SEM photographs of the dendritic Pt film (a) before the reduction treatment, (b) after the reduction treatment.



Fig. 3. TEM photographs of the dendritic Pt film at the magnitude of $\times 100,000$.

sity of the dendritic Pt film is 3.3 g cm^{-3} . When considering that the bulk Pt density is 21.45 g cm^{-3} , this dendritic Pt film has very low density without using any support material. Fig. 4 displays the SEM micrograph of the conventional sputtered Pt film in which

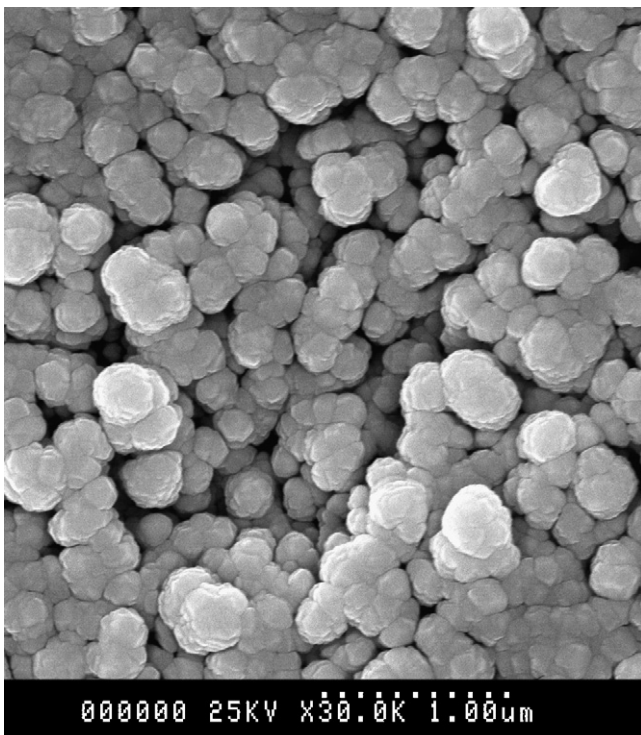


Fig. 4. SEM image of the conventional Pt catalyst sputtered on MPL surface.

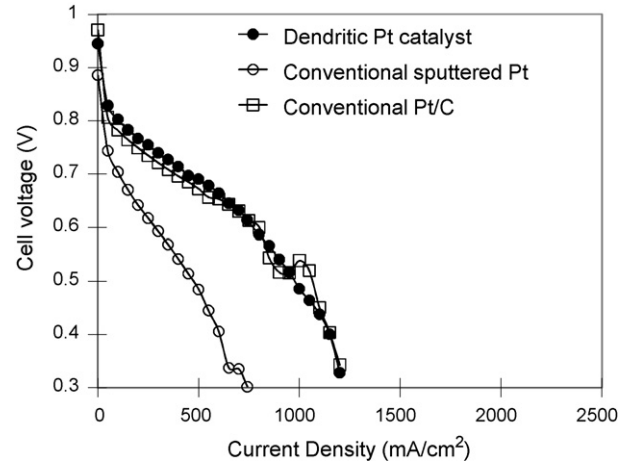


Fig. 5. Single cell performances for H_2/Air operation at 80°C of the dendritic Pt, the conventional Pt catalyst, and the conventional Pt/C.

the agglomeration of large Pt particles is observed. The evaluated density of the conventional sputtered Pt film is about 13.2 g cm^{-3} , which is 4 times higher than that of the dendritic Pt film.

3.2. Fuel cell performance

Fig. 5 shows the current-voltage characteristics of the each unit cell, employing each catalyst for the cathode. As obvious from this figure, the dendritic Pt catalyst film shows higher performance than that of the conventional sputtered Pt film, and almost equal to that of the Pt/C. The current densities in the maximum current region are compared, resulting in 1200 mA cm^{-2} or more for the cell with the dendritic Pt catalyst and 740 mA cm^{-2} for that with the conventional catalyst. That is, the dendritic Pt film possess improved mass transport performance in the catalyst layer compared to the conventional sputtered Pt layer.

Fig. 6 shows the current-voltage characteristics of each unit cell. The performance of the dendritic Pt catalyst is high in all the current density regions compared to the conventional sputtered Pt catalyst and the Pt/C. This figure also shows that the O_2 gain of the dendritic Pt catalyst is lower than that of conventional sputtered Pt layer. The O_2 gains of the dendritic Pt, the conventional sputtered Pt and the Pt/C are 57 mV, 147 mV and 44 mV at 400 mA cm^{-2} respectively.

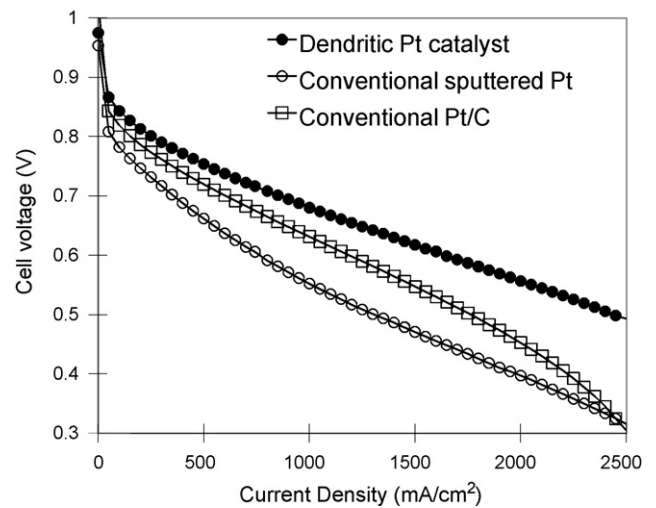


Fig. 6. Single cell performances for H_2/O_2 operation at 80°C of the dendritic Pt, the conventional Pt catalyst, and the conventional Pt/C.

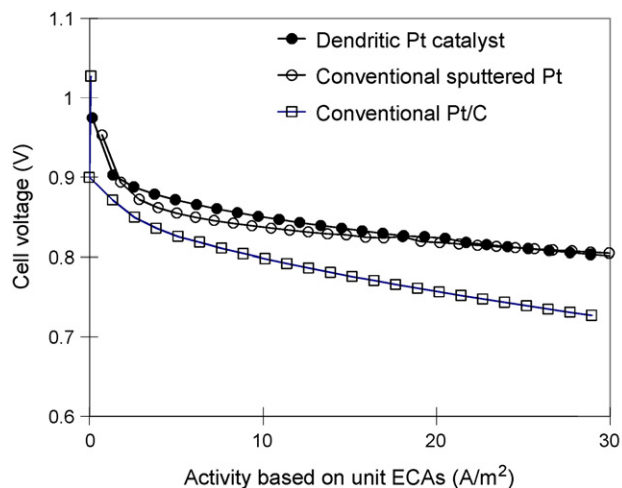


Fig. 7. Comparison of activities based on unit ECAs between the dendritic Pt, the conventional Pt catalyst, the conventional Pt/C.

The specific ECA of the dendritic Pt catalyst, the conventional sputtered Pt catalyst and the Pt/C are about 14 , $3 \text{ m}^2 \text{ g}^{-1}$ and $53 \text{ m}^2 \text{ g}^{-1}$, respectively. These results indicate that the dendritic structure provides improved diffusion characteristics and larger ECA compared with the conventional sputtered Pt layer, and almost the same diffusion performance as the Pt/C catalyst.

Fig. 7 shows the activities based on unit ECAs of each cathode catalyst, calculated from the specific ECA and the performances displayed in Fig. 6. It is found that the activity of the dendritic Pt is higher compared to the Pt/C, and almost equal to the conventional sputtered Pt catalyst. These results mean that the dendritic Pt catalyst has higher ECA and diffusion performance than that of the

conventional sputtered Pt catalyst, and higher Pt utilization in the electrochemical interface compared to Pt/C.

4. Conclusions

Pt catalyst with dendritic structure was formed through a reactive sputtering process, and its catalytic performances applied to the cathode of PEFC were evaluated. Despite using no support material, this dendritic Pt catalyst exhibited a very low density of 3.3 g cm^{-3} and a high Pt utilization in the electrochemical interface. The dendritic structure provided improved diffusion characteristics and larger ECA compared to a conventional sputtered Pt film. This dendritic Pt film seems to be a promising cathode catalyst, but further investigation is needed to improve the properties, such as a low mass specific ECA compared to the Pt/C. Future efforts including the careful evaluation of durability are also currently in progress.

References

- [1] Y. Shao, G. Yin, Y. Gao, *J. Power Sources* 171 (2007) 558.
- [2] E. Antolini, *J. Mater. Sci.* 38 (2003) 2995.
- [3] S.Y. Cha, W.M. Lee, *J. Electrochem. Soc.* 146 (1999) 4055.
- [4] R. O'Hayre, S.J. Lee, S.W. Cha, F.B. Prinz, *J. Power Sources* 109 (2002) 483.
- [5] A. Bonakdarpour, R. Lobel, S. Sheng, T.L. Monchesky, J.R. Dahn, *J. Electrochem. Soc.* 153 (12) (2006) A2304.
- [6] D. Gruber, N. Ponath, J. Muller, F. Lindstaedt, *J. Power Sources* 150 (2005) 67.
- [7] J. Zhensheng, X. Chanjuan, Z. Qingmei, Y. Feng, Z. Jiazhen, Z. Jinzhen, *J. Mol. Catal. A: Chem.* 191 (2003) 61.
- [8] M.C. Jung, H.D. Kim, M. Han, W. Jo, D.C. Kim, *Jpn. J. Appl. Phys.* 38 (1999) 4872.
- [9] H. Neff, S. Henkel, E. Hartmannsgruber, E. Steinbeiss, W. Michalke, K. Steenbeck, H.G. Schmidt, *J. Appl. Phys.* 79 (1996) 7672.
- [10] M. Hecq, A. Hecq, J.P. Delrue, T. Robert, *J. Less-common Met.* 64 (1979) 25.
- [11] J.R. McBride, G.W. Graham, C.R. Peters, W.H. Weber, *J. J. Appl. Phys.* 69 (1991) 1596.
- [12] Y. Abe, H. Yanagisawa, K. Sasaki, *Jpn. J. Appl. Phys.* 37 (1998) 4482.
- [13] Y. Abe, H. Yanagisawa, K. Sasaki, *Jpn. J. Appl. Phys.* 38 (1999) 2092.